Giant dispersive wave generation through soliton collision

M. Erkintalo, G. Genty, J.M. Dudley

Giant dispersive wave generation through soliton collision

M. Erkintalo,[1] G. Genty,[1,*] and J. M. Dudley[2]

[1]*Department of Physics, Tampere University of Technology, FI-33101 Tampere, Finland*
[2]*Institut FEMTO-ST, UMR 6174 CNRS-Université de Franche-Comté, Besançon, France*
**Corresponding author: goery.genty@tut.fi*

We numerically study long pulse supercontinuum generation in a photonic crystal fiber with two zero-dispersion wavelengths, reporting a dynamical effect where soliton collisions excite dispersive waves with 1 order of magnitude greater peak power than that arising from single-soliton generation. The dispersive wave peak power exhibits extreme-value "rogue" characteristics, with the long tail of the distribution populated by collision-related events.

Supercontinuum (SC) generation in a photonic crystal fiber (PCF) with two zero-dispersion wavelengths (ZDWs) can lead to novel dynamics owing to the influence of a negative dispersion slope on soliton propagation [1–3]. A particular effect when pumping between the ZDWs in the anomalous dispersion regime using femtosecond pulses is the stabilization of the Raman self-frequency shift when solitons ejected from the SC approach the second ZDW and shed energy through dispersive wave radiation into the long-wavelength normal dispersion regime. The dynamics of this process is preserved even with long pulse pumping in the picosecond and cw regime [4,5]. Long-pulse SC generation has also been of recent interest, because the development of the SC from noise-induced modulation instability (MI) leads to large amplitude optical rogue wave or "rogue soliton" fluctuations [6–10]. In this Letter, we report on a feature of long pulse SC generation in a PCF with two ZDWs, whereby collisions between solitons with different wavelengths induce the generation of extremely large-amplitude "giant" dispersive waves (DWs) in the normal dispersion regime. Such collision-induced DWs are rare, but they can have peak power more than 1 order of magnitude larger than those emitted by single solitons. The distribution of the DW peak power exhibits the L-shape characteristic of rogue wave statistics, and we confirm that the extended tail of the distribution arises from the collision-induced events.

Our simulations consider SC generation in a commercially available PCF (Crystal Fibre NL-PM-750) with ZDWs at 790 nm and 1260 nm. Figure 1 shows the dispersion profile, and we used a nonlinear coefficient $\gamma = 0.1\ \mathrm{W^{-1}m^{-1}}$ at a 900 nm pump wavelength. We simulate 200 W peak power, 4 ps FWHM sech^2 pulses propagating in 1.8 m of PCF using standard numerical techniques to solve the generalized nonlinear Schrödinger equation [5]. Modeling includes the Raman effect, the frequency-dependent effective area, and a one-photon-per-mode noise background. To study the DW stochastic properties, we generated an ensemble of 1000 simulations using different noise seeds.

Our results show spectra spanning from 800−1400 nm, but the effect of noise yields significant differences in structure between different realizations in the ensemble. Figure 1 plots two particular results: Fig. 1(a) shows an event close to the median SC broadening, associated with an emitted DW around 1500 nm, while Fig. 1(b) shows a rare event in the ensemble where the DW extends significantly further to a longer wavelength around 1540 nm. Significantly, inspecting the corresponding temporal profiles (filtering above 1400 nm) shows that the peak power of the DW associated with the extended spectrum exceeds by 1 order of magnitude that of the low-power median case.

The results in Fig. 1(b) are unexpected, because the DW peak power when generated by a resonantly phase-matched single soliton typically decreases with wavelength shift into the normal dispersion region [11]. To investigate the origin of the high-amplitude

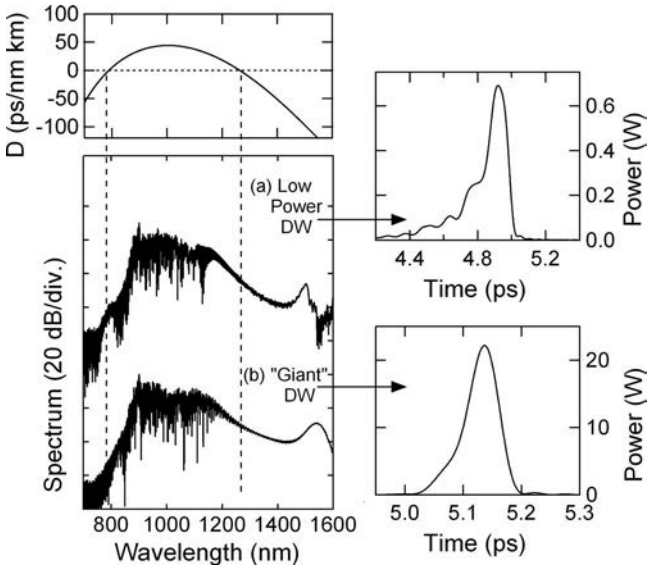

Fig. 1. Spectra and temporal profiles of DW components for two events in the ensemble: (a) a low-power DW and (b) a giant DW associated with a soliton collision. The spectra are referred to the dispersion curve (top) with the dashed lines indicating the ZDWs.

DWs in more detail, we carefully examined the spectral and temporal characteristics of all the results in the ensemble. To this end, we (i) performed numerical filtering to isolate the DW components in the normal dispersion regime above 1400 nm then (ii) determined the wavelength of maximum amplitude and the peak power of the corresponding temporal pulse. Figure 2(a) plots these results, and we clearly see a clustering of generated DWs that follow the expected trend where increased wavelength shift is associated with reduced peak power. However, we also see a secondary population of events where the peak power at a given wavelength is significantly displaced relative to the region of heavy clustering. Indeed, we note a very small number of events at a much higher peak power (20–60 W) and/or larger detuning into the normal dispersion region (1500–1600 nm). Figure 2(b) plots the corresponding peak power histogram, showing that the high-power events with peak powers exceeding 20 W lead to a significantly extended distribution tail.

Further analysis allows us to identify very different propagation dynamics associated with these two classes of events. In particular, we find that higher peak power DWs in the scatter plot in Fig. 2(a) do not arise from single-soliton dynamics, but they instead involve the collision between two solitons emerging from the noisy SC. Our analysis was based on manual inspection of the evolution and/or output spectrograms for each run in the ensemble, where the time-frequency dynamics clearly show the difference between single soliton and collision induced events (see also Fig. 4). This is because a collision generates a DW only at the point of collision and at a wavelength far from the ZDW, whereas single-soliton DW generation around the second ZDW occurs over an extended propagation distance [1]. We also note that the presence of the second ZDW significantly modifies the single-soliton dynamics [10] such that rogue wave statistics as in [6] are not observed here. Figure 2(a) distinguishes the DWs generated by single solitons (black circles) from those generated as a result of soliton collisions [gray circles (red online)], and it is clear that the higher amplitude events are generated only from the effect of collisions. This is a significant observation in that it allows us to associate a particular physical process (soliton collision) with the generation of the high-power events in the tail of the associated histograms.

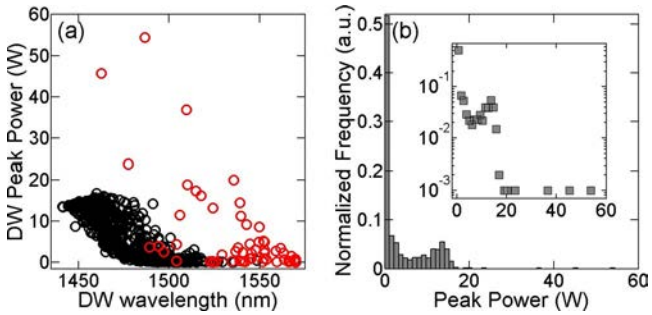

Fig. 2. (Color online) (a) Scatter plot of DW peak power versus wavelength for all results in the ensemble using filtering above 1400 nm. Black circles are events from single-soliton DW generation. Gray circles (red online) are events from soliton collisions. (b) Corresponding histogram plotting DW peak power distribution.

Figure 3 shows the mechanism of collision-induced DW generation in more detail. Here we consider the case of Fig. 1(b), but we have checked that near-identical propagation dynamics are observed for all events indicated by gray circles in Fig. 2(a). Figure 3(a) plots the temporal evolution, illustrating how initial MI on the pulse envelope leads to a series of periodic subpulses (emerging around 0.5 m), which recent work has shown can be described in terms of Akhmediev breathers [12]. Beyond this distance, the breather structures subsequently evolve into distinct solitons, and it is the dynamics in this phase of evolution that yields the collision events of interest. The inset highlights one particular collision, and Fig. 3(b) shows a more detailed view to illustrate the significantly higher field intensity attained as a result. The simultaneous emission of a strong DW is also clearly seen.

We obtain further insight by examining the collision process in the time-frequency domain. Figure 4 plots the calculated spectrograms around the point of collision, using a 200 fs gate function to more clearly isolate the spectral dynamics. The corresponding temporal intensity profiles (spanning 300 fs) are plotted alongside. At 1.6 m prior to the collision [Fig. 4(a)], we see two 30 fs FWHM solitons with 100 fs separation. The solitons have central wavelengths of 1090 and 1140 nm, but their 45 nm bandwidths mean that they spectrally overlap, resulting in spectral modulation as seen in the figure. Their different group velocities yield a collision at 1.7 m [Fig. 4(b)], and we see how the superposition field is compressed to 15 fs, with peak power over four times higher than the individual solitons before and after the collision in Figs. 4(a) and 4(c). Significantly, this allows us to physically interpret the generation of the large-amplitude DW in terms of both increased power of the superposition field and increased spectral extension into the normal dispersion regime. This is in contrast to collision-induced DWs as in [3], where the collision plays an indirect role by enhancing the redshift experienced by one of the solitons which then emits a DW near the fiber output.

We stress that no radiation is emitted by individual solitons before or after the collision, and thus the large amplitude DW can be unambiguously attributed to the collision. This is because the indi-

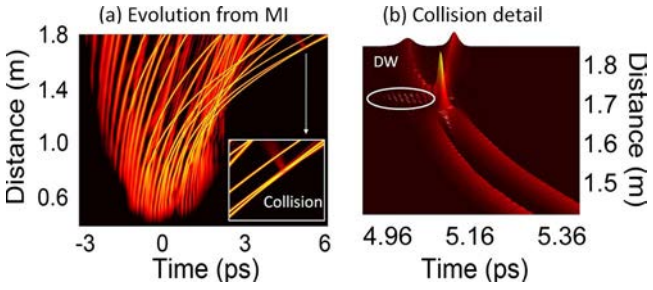

Fig. 3. (Color online) (a) Temporal evolution showing how MI is followed by soliton emergence. The inset in (a) and the 3D plot in (b) show a collision event in more detail.

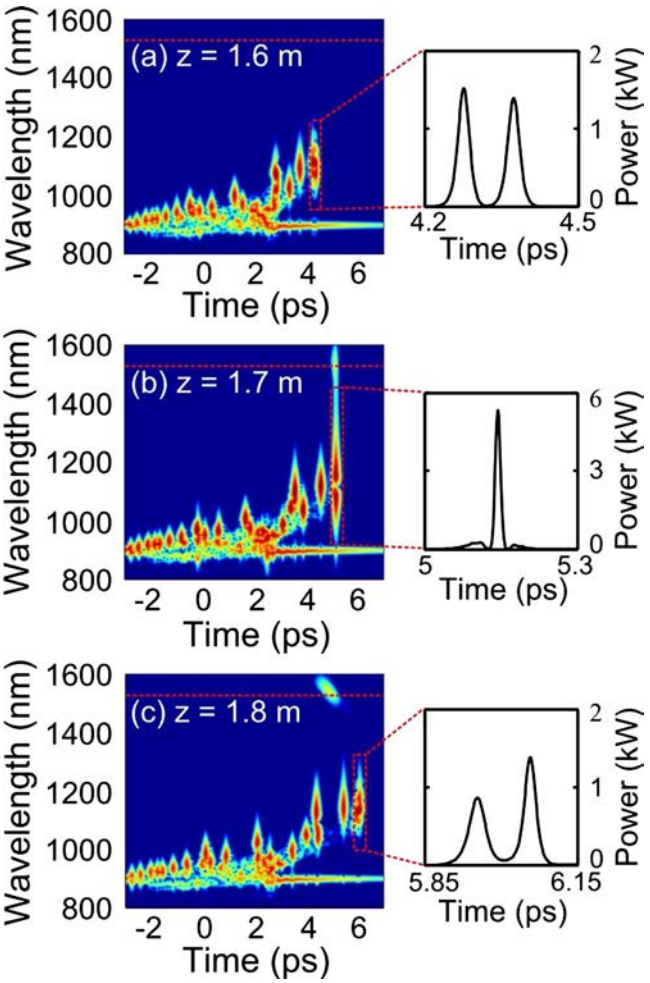

Fig. 4. (Color online) Spectrograms at propagation distances as shown to illustrate collision-induced DW generation in the time-frequency domain. The spectrogram gate function was 200 fs duration. The dashed line above 1500 nm shows the calculated phase-matching wavelength as described in the text.

vidual soliton wavelengths before and after the collision are too far from the ZDW to phase match DW generation; it is precisely the increase in bandwidth and peak power during the collision that allows the DW phase-matching condition to be satisfied. Also in this context, we note that the peak power and wavelength of the giant DW are determined by both the peak power and wavelength of the collision field. In fact, we have checked that the DW wavelength is accurately predicted if one uses the standard phase-matching condition for DW generation using the peak power of the soliton superposition field attained during the collision and center wavelength taken as the most redshifted of the colliding solitons. These are shown as the dashed lines above 1500 nm in Fig. 4.

Of course the distance at which the collision occurs also influences the output DW peak power, because DWs generated earlier disperse over a greater distance and have reduced peak power at the fiber output. In general the collision-induced DWs detected at the fiber output exhibit a peak power, which is a decreasing function of the observed wavelength shift both because the collisions yielding DWs at larger wavelength shifts typically occur at shorter propagation distances and because DWs generated further from the ZDW experience larger dispersion. In contrast, only a small number of soliton collisions occur between solitons closer to the ZDW near the fiber output, explaining the rarity of DW events with the highest peak powers.

Our results here have demonstrated the process of soliton collision-induced giant DW generation in a PCF with two ZDWs. The corresponding peak power distribution exhibits extreme-value statistics, and a significant feature of our results has been the unambiguous association of these "rogue" events with the collision dynamics. Although we have discussed the generation of such rogue dispersive waves at longer wavelengths beyond the second ZDW point, a similar effect should in principle be observed on the short-wavelength normal dispersion regime, or even in the case of a fiber with single ZDW. Our results also suggest that when accompanied by numerical simulations, the statistical analysis of DW amplitude and wavelength may provide a useful signature of the presence of soliton collisions in noisy SC generation even when direct measurements are not possible.

We thank the Academy of Finland (research grants 121953, 130099, and 132279), the Institut Universitaire de France, and the French Agence Nationale de la Recherche project MANUREVA (ANR-08-SYSC-019) for support.

References

1. D. V. Skryabin, F. Luan, J. C. Knight, and P. St. J. Russell, Science **301**, 1705 (2003).
2. G. Genty, M. Lehtonen, H. Ludvigsen, and M. Kaivola, Opt. Express **12**, 3471 (2004).
3. F. Luan, D. V. Skryabin, A. V. Yulin, and J. C. Knight, Opt. Express **14**, 9844 (2006).
4. A. Mussot, M. Beaugeois, M. Bouazaoui, and T. Sylvestre, Opt. Express **15**, 11553 (2007).
5. J. M. Dudley, G. Genty, and S. Coen, Rev. Mod. Phys. **78**, 1135 (2006).
6. D. R. Solli, C. Ropers, P. Koonath, and B. Jalali, Nature **450**, 1054 (2007).
7. J. M. Dudley, G. Genty, and B. J. Eggleton, Opt. Express **16**, 3644 (2008).
8. M. Erkintalo, G. Genty, and J. M. Dudley, Opt. Lett. **34**, 2468 (2009).
9. A. Mussot, A. Kudlinski, M. Kolobov, E. Louvergneaux, M. Douay, and M. Taki, Opt. Express **17**, 17010 (2009).
10. B. Kibler, C. Finot, and J. M. Dudley, Eur. Phys. J. Spec. Top. **173**, 289 (2009).
11. N. Akhmediev and M. Karlsson, Phys. Rev. A **51**, 2602 (1995).
12. J. M. Dudley, G. Genty, F. Dias, B. Kibler, and N. Akhmediev, Opt. Express **17**, 21497 (2009).